Engineering Notes

ENGINEERING NOTES are short manuscripts describing new developments or important results of a preliminary nature. These Notes cannot exceed 6 manuscript pages and 3 figures; a page of text may be substituted for a figure and vice versa. After informal review by the editors, they may be published within a few months of the date of receipt. Style requirements are the same as for regular contributions (see inside back cover).

Skylab Detection of an Algal Bloom in the Gulf of Mexico

William R. Johnson*
Lockheed Electronics Company, Inc., Houston, Texas
and
Dean R. Norris†
Florida Institute of Technology, Melbourne, Fla.

Introduction

SKYLAB multispectral scannner data were used to study the spectral characteristics of an algal bloom in the Gulf of Mexico. Radiance profiles of the water and algae were prepared with data from 10 bands of a scanner covering the spectral range from 0.42 to 2.35 μm. The high response in the near-infrared spectral bands implies a possible classification and discrimination parameter for detection of phytoplankton blooms.

Event and Data Sources

On Jan. 21 1974 at 2012 GMT, Skylab acquired photographic camera systems (S190A, S190B) and multispectral scanner (S192) data over the Gulf of Mexico, about 110 km west of Fort Myers, Florida (Fig. 1). At 1800 GMT, 2 hours prior to the passage of Skylab, a C-130 aircraft flew over this portion of the Skylab track at an altitude of 800 m and photographed the ocean surface with an RC-8 camera system. Aircraft observers noted an algal bloom in the water at various segments of the route.

Weather observations made by ships in the eastern Gulf of Mexico, as well as by nearby land stations, indicated the environment in the bloom area to be surface winds from the south at 4—5 m/s (8—10 knots); air temperature/dew point, 27/22°C (80/72°F); and water temperature, 24.2—25°C (75—77°F). At Skylab pass time, the Sun elevation angle was 31.5 deg., and the Sun azimuth was near 222 deg.

The Skylab Earth Resources Experiment Package (EREP) sensors used in this study consisted of the S190B Earth terrain camera (ETC) and the S192 multispectral scanner.[1] The ETC transparency had a ground resolution of 15 m per line pair. The S192 operated in 13 discrete bands from 0.4 to 12.5 μm. The conical scan of the S192 resulted in the Earth's surface being viewed through an atmospheric path of the same length in all parts of the scan. Thus, atmospheric corrections are uniform across the image.

Data from the aircraft consisted of photography from the RC-8 camera, and observations from the crew and scientists who were on board. These observations confirmed the visual aspects and extent of the phenomena.

Data Analysis and Results

Figure 1 (showing S190B photo and S192 scan limits) outlines the area of analysis. The high-quality transparency from the ETC camera shows, by use of a magnifying eyepiece, that the algae extended about 120 km along the track and can be seen in various patterns and concentrations. The most prominent concentration, slightly west of the track, was about 20 km long. It was also in a position to be recorded by the S192 in 10 of the 12 narrow bands from 0.42 to 2.35 μm and in one 10.2 to 12.5 μm thermal band. Imagery in each band was screened and analyzed on the Passive Microwave Imagery System, Display Analysis Station (PMIS, DAS),[2] In the imagery of the higher visible (0.6—0.7 μm) and near-infrared (0.7—1.1 μm) wavelengths, a significant contrast was seen between the algal blooms and the water. There was only slight contrast seen in the imagery of the lower three visible bands (less than 0.55 μm) and above about 1.6 μm. An image (Fig. 2) of the algae using band 7 (0.78—0.88 μm) shows the individual data points used in electronic data processing. The image is generated by scaling grey values to the intensity of the signal recorded for this wavelength, thus visually maximizing the contrast between the algae and surrounding water.

After selecting representative samples of spectral data from within the algal bloom feature and data from a control water area believed clear of algae (located approximately 7 km northwest of the feature), the absolute radiance values were computed at each of the 10 available spectral bands in the visible and infrared ranges. The spectral plots of the algal radiance and the control water radiances are shown in Fig. 3 as a solid (top) line and a dashed (middle) line, respectively. The dotted (bottom) line represents the radiance emitted from the sea as it would be measured immediately above the surface, having subtracted out the effect of atmospheric back scatter[3] and neglecting surface reflection, and shows that the water absorbs all of the incident infrared solar irradiance; no spectral radiance above 0.74 μm would be measurable. The area between the dotted and dashed curves is representative of the solar energy scattered back to space by the atmosphere. The area between the solid and dashed curves represents the added energy reflected by the algal bloom.

Discussion

Examination of the shaded area (Fig. 3) representing the algal radiance reveals that the surface reflectances of the two sample areas vary considerably. The algal spectral radiance from 0.55 to 1.1 μm is significantly higher than that of the control water, with the 0.7- to 0.9-μm portion of the spectrum having the greatest potential for remotely sensing the algal bloom. Since the water is a strong absorber above 0.74 μm, the bloom must be a surface phenomenon. Because of the distance from the shore and the relatively high surface reflectance, it is believed that this bloom was *Oscillatoria* (*Trichodesmium*) *erythraea,* a blue-green alga known to bloom at the surface of oceanic waters.

Although no spectral profiles were presented, a blue-green (*Aphanizomenon flos-aquae*) algal bloom in Utah Lake has been recorded from space and documented by surface truth.[4] Spectrometric profiles of various algal (chlorophyll) concentrations have been recorded from aircraft.[5-8] Though not consistent, these data generally show a higher reflectance, at least above about 0.5 μm, for higher algal concentrations.

Presented as Paper 77-1565 at the AIAA/AGU/AMS/IEEE/MTS/SEG Conference on Satellite Applications to Marine Operations, New Orleans, La., Nov. 15-17, 1977; submitted Jan. 9, 1978; revision received May 3, 1978.

Index categories: Oceanography, Physical and Biological; Aerospace Technology Utilization.

*Senior Scientist, Earth Observations Dept., Systems and Services Div.

†Associate Professor, Dept. of Oceanography and Ocean Engineering.

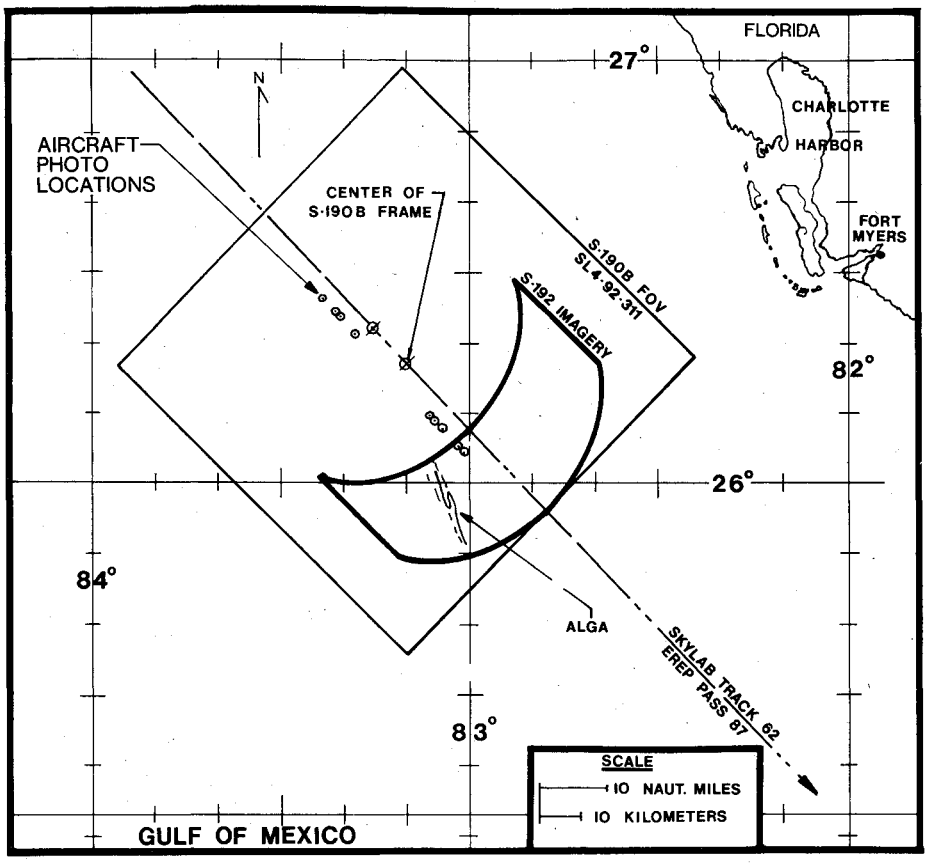

Fig. 1 Gulf of Mexico map showing area coverage of Skylab and aircraft imagery.

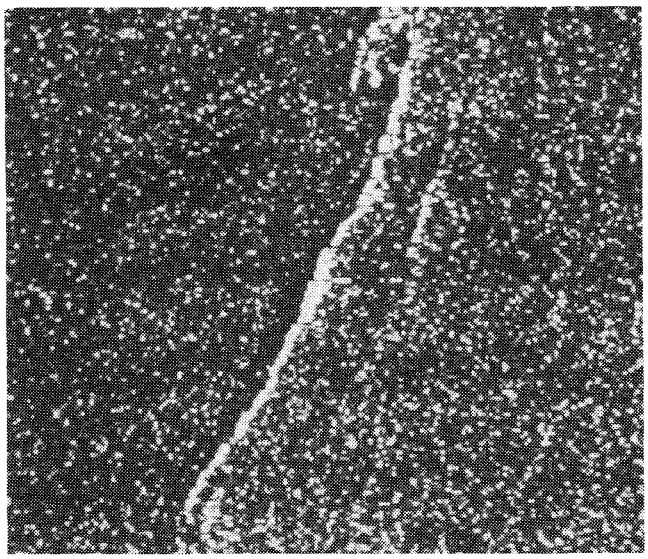

Fig. 2 Skylab S192 imagery of band 7 (0.78—0.88 μm).

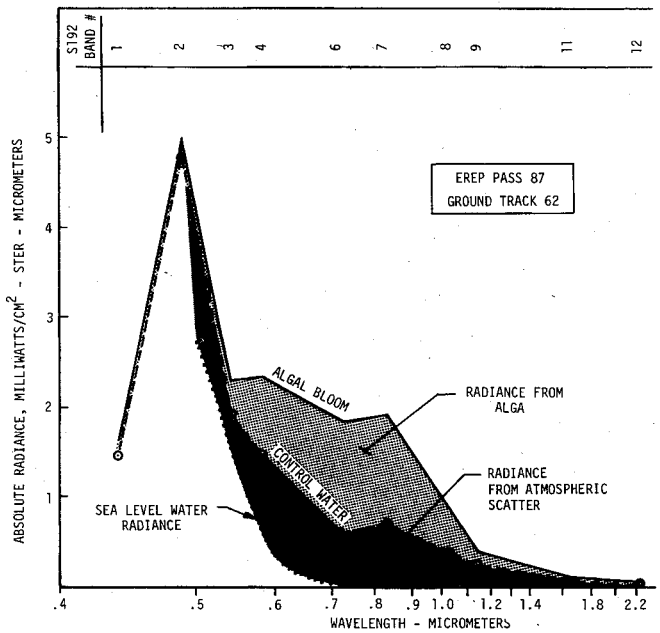

Fig. 3 Spectral profiles of the absolute radiance of algae and control water using data from S192 bands.

Upwelling irradiance spectra taken from 4 m above the sea surface also indicate a higher reflectance above 0.5 μm for a plankton bloom.[9]

Conclusion

Skylab's high-resolution camera system (ETC) was used to confirm the extent of a marine algal bloom across the path of the aircraft which photographed the area nearly simultaneously. The multispectral scanner data and imagery provided opportunity to study the reflected energy from the algae, and to show the high reflectivity in the 0.7- to 0.9-μm portion of the spectrum. Although the surface truth consists of aircraft crew sightings, the evidence presented confirms the occurrence of a marine algal bloom, illustrates the role of remote sensing in identifying algal blooms, and confirms the feasibility of using space-acquired data to monitor the existence and extent of phytoplankton blooms.

Acknowledgment

Support for this report was provided by the National Aeronautics and Space Administration, Lyndon B. Johnson Space Center, Science and Applications Directorate, Houston, Texas, under Contract NAS 9-15200.

References

[1] *Skylab EREP Investigators Information Book*, MSC-07874, NASA/JSC, April 1973.

[2] "Operational Procedure For Passive Microwave Imagery System (PMIS)," NASA/JSC, CAD 2584-8, 1975.

[3] Rainey, D.A., Johnson, W.R., and Wilmarth, V.R., "The Skylab S191 Spectrometer Experiment," TM58208 (JSC-13886), NASA/JSC, 1978, pp. 11-21.

[4] Strong, A.E., "Remote Sensing of Algal Blooms by Aircraft and Satellite in Lake Erie and Utah Lake," *Remote Sensing of Environment*, Vol. 3, 1974, pp. 99-107.

[5] Clarke, G.L., Ewing, G.C., and Lorenzen, C.J., "Spectra of Backscattered Light From the Sea Obtained From Aircraft as a Measure of Chlorophyll Concentration," *Science*, Vol. 167, 1970, pp. 1119-1121.

[6] Maul, G.A., "Remote Sensing of Ocean Currents Using ERTS Imagery," Goddard Space Flight Center, Greenbelt, Md., NASA SP-327, 1973, pp. 1365-1375.

[7] Mueller, J.L., "The Influence of Phytoplankton on Ocean Color Spectra," Ph.D. Thesis, School of Oceanography, Oregon State University, Corvallis, Oregon, 1974.

[8] Clarke, G.L. and Ewing, G.C., "Remote Sensing of Ocean Color as an Index of Biological and Sedimentary Activity," *Proceedings of the Symposium COSPAR Approaches to Earth Survey Problems Through Use of Space Techniques*, Akademie Verlag, Berlin, 1974, pp. 101-120.

[9] Maul, G.A., "Applications of ERTS Data to Oceanography and the Marine Environment," *Proceedings of the Symposium COSPAR Approaches to Earth Survey Problems Through Use of Space Techniques*, Akademie Verlag, Berlin, 1974, pp. 335-347.

Simple Numerical Model for Calculation of Entry Vehicle Trim Response

Thomas D. Burton*

Washington State University, Pullman, Wash.

THE influence of mass and configurational asymmetries on the dynamics of slender, spinning entry vehicles is an important aspect of vehicle design and performance assessment. High-altitude roll resonance and lower-altitude roll/trim effects influence vehicle loading and attendant impact miss. Descriptions of aerodynamic trim effects on re-entry vehicle (RV) angle of attack for vehicles with linear aerodynamics are well known.[1-4] Influence of nonlinear aerodynamics on resonant and nonresonant response have been considered by Murphy[5] and by Nayfeh and Saric.[6,7] Although these solutions are useful in characterizing angle-of-attack response, it is still generally necessary to numerically integrate the six-degree-of-freedom equations of motion in order to quantify the resulting trim-induced dispersion for a given re-entry system. This is often done using a Monte Carlo approach, necessitating significant amounts of computer time.

Presented in this Note is a simple trim response model which is numerically efficient and which can be incorporated into standard point-mass trajectory simulators for calculation of trim-induced dispersion and angle-of-attack/load behavior. This model is based on the fact that the coupling of trim and body fixed low-frequency (in the sense of Nelson[8]) oscillatory motion component dominates the trim-induced response. The high-frequency component/trim coupling is not significant, except in cases where sudden trim changes are encountered, e.g., due to rapid configurational change. By using standard asymptotic solutions to linear differential equations with time varying coefficients,[9] the two second-order equations in angle-of-attack α and sideslip β can be reduced to two first-order equations in which the high-frequency contribution is eliminated. This allows for a much coarser integration increment in calculating the trim-induced response.

In the present model, time variations in roll rate, asymmetries, and aerodynamic coefficients are taken into account. Longitudinal principal axis misalignments in pitch and yaw are also included, which was not done in the previously cited work.[1-7] In addition to the reduced equations of motion, results are obtained for the effect of roll acceleration and so-called density damping on the steady-state trim angle relations. The simplified model is shown to provide adequate accuracy in calculating the combined low-frequency/trim contribution to angle-of-attack.

The angle-of-attack behavior is formulated in body fixed coordinates as used by Nelson.[8] For small angles of attack, linear aerodynamics, and with inclusion of products of inertia and aerodynamic asymmetries for an otherwise symmetric vehicle, the equations of rotational motion may be written as follows:

$$\dot{\beta} = -r + p\alpha - (q_\infty S C_{L_\alpha}/mV)\beta \tag{1}$$

$$\dot{\alpha} = q - p\beta - (q_\infty S C_{L_\alpha}/mV)\alpha \tag{2}$$

$$\dot{q} = (1 - A/B)pr + (q_\infty Sd/B)[C_{m_\alpha}\alpha + (d/2V)C_{m_q}q + C_{m_0}] - \epsilon_3(1 - A/B)p^2 \tag{3}$$

$$\dot{r} = -(1 - A/B)pq + (q_\infty Sd/B)[-C_{m_\alpha}\beta + (d/2V)C_{m_q}r + C_{n_0}] + \epsilon_2(1 - A/B)p^2 \tag{4}$$

$$\dot{p} = (q_\infty Sd/A)C_l \tag{5}$$

Here, α and β are angles of attack and sideslip, respectively; p, q, and r are roll, pitch, and yaw rates, respectively; A and B are roll and pitch moments of inertia (pitch and yaw moments of inertia are assumed equal); vehicle mass and aerodynamic reference area and length are denoted by m, S, and d, respectively. Dynamic pressure is $q_\infty = \frac{1}{2}\rho V^2$, where ρ is atmospheric density and V is vehicle velocity. $C_{m\alpha}$, C_{mq}, $C_{L\alpha}$, and C_l are aerodynamic coefficients of static stability, dynamic stability, lift, and roll torque. C_{m0} and C_{n0} are aerodynamic trim-producing asymmetries in pitch and yaw, while ϵ_3 and ϵ_2 are pitch and yaw misalignments of the longitudinal principal axis.

Equations (1-4) can be combined into a single second-order equation in complex angle-of-attack $\xi = \beta + i\alpha$, written in the following form:

$$\ddot{\xi} + (2i\Delta\omega - 2\lambda_0)\dot{\xi} + (\omega^2 + 2i\lambda_1)\xi = T_0 \tag{6}$$

where

$$\Delta\omega = p(1 - A/2B)$$

$$\lambda_0 = -(q_\infty S/mV)[C_{L_\alpha} - (md^2/2B)C_{m_q}]$$

$$\lambda_1 = (pq_\infty S/2mV)[(1 - A/B)C_{L_\alpha} - (md^2/2B)C_{m_q}] + \dot{p}$$

$$\omega^2 = -(q_\infty Sd/B)C_{m_\alpha} - (1 - A/B)p^2$$

$$T_0 = N_0 + iM_0$$

$$M_0 = (q_\infty SdC_{m_0}/B) + \epsilon_3(1 - A/B)p^2$$

$$N_0 = -(q_\infty SdC_{n_0}/B) + \epsilon_2(1 - A/B)p^2$$

Received March 6, 1978; revision received May 9, 1978.

Index category: LV/M Dynamics and Control.

*Assistant Professor, Department of Mechanical Engineering. Member AIAA.